

# Registration and aliasing

LE TRAN Ngoc Tran \*

Université de Paris

December 27, 2021

## Abstract

In this work, we analyse the influence of aliasing, noise and registration method on registration accuracy. First, we show that some reduction methods which transform periodic images into reduced images may cause aliasing. This reduce the accuracy of the image registration. In this case, Gaussian smoothing can help to reduce the effects of aliasing and thus improve the accuracy of the image registration. In term of the interpolation method for image registration, we realize that the Shannon interpolation give more accurate result than the bilinear interpolation.

## Contents

<b>1</b>	<b>Introduction</b>	<b>1</b>
<b>2</b>	<b>Reduction methods</b>	<b>2</b>
2.1	Strong aliasing scenario (direct subsampling) . . . . .	3
2.2	Light aliasing scenario without no frequency cut off . . . . .	3
2.3	No aliasing scenario with hard frequency cut off . . . . .	5
<b>3</b>	<b>Registration methods</b>	<b>6</b>
3.1	Bilinear interpolation . . . . .	6
3.2	Shannon interpolation . . . . .	7
<b>4</b>	<b>Numerical results</b>	<b>10</b>
4.1	The recurrent testing pattern . . . . .	10
4.2	Test case with bilinear interpolation . . . . .	10
4.3	Test case with Shannon interpolation . . . . .	11
4.4	Test case with Shannon interpolation and Gaussian smoothing . . . . .	12
<b>5</b>	<b>Conclusion</b>	<b>13</b>

## 1 Introduction

Image registration is a process of overlaying images (two or more) to combine information from several images which are taken at different time, from different view points or different sensors. It involves mapping points from one image to corresponding points in another image. It is used in many application such as computer vision, medical image and compiling and analyzing images from satellites. In this work, we restrict our

---

\*tran.le-tran-ngoc@etu.u-paris.fr

study to the translation between the register and reference image.

If no aliasing, it is well known that reduction and translation can commute which means  $R_z(T_t u_1) = T_t(R_z u_1)$ . It implies that we can perform the image registration for the reduction images with no loss for the accuracy. This is a crucial point to reduce the computational cost of the image registration process. However, some reduction methods as direct subsampling can cause the aliasing problem. This gives an effect on the accuracy of registration method. In this work, we would like to investigate the impact of the reduction methods on the accuracy of the registration method in term of noise and without noise.

The rest of this work is organized as follows: we give some short description of the reduction methods which consist of strong, light and no aliasing scenario in Section 2. Next, we discuss the Bilinear interpolation and Shannon interpolation for the image registration methods in Section 3. With Bilinear interpolation, we show that we can explicitly derive the exact algorithm for the translation between two images by simply solving a linear least square problem. For the Shannon interpolation, the images registration based on the cross correlation between two images leads to an equivalent problem which is to find the maximal sup-pixellic position. A fast subpixel registration algorithm is also presented in this section. The recurrent testing pattern and numerical results is investigated in Section 4 to illustrate our purposes. Finally, in Section 5, we draw some conclusions and relevant direction for the future work.

## 2 Reduction methods

In this part, we list some methods to reduce the dimensionality of data which called reduction methods. Depends on each method that the reduced images has strong or light or no aliasing. All the reduction methods were implemented in Fourier domain. First, we recall:

For a square image of size  $N \times N$ , the two-dimensional Discrete Fourier Transform (DFT) is given by:

$$F(k, l) = \sum_{i=0}^{N-1} \sum_{j=0}^{N-1} f(i, j) e^{-i2\pi(\frac{ki}{N} + \frac{lj}{N})} \quad (1)$$

where  $f(a, b)$  is the image in the spatial domain and the exponential term is the basis function corresponding to each point  $F(k, l)$  in the Fourier space.

Notice that  $u_0$  is the periodic image we use to this part to implement reduction images. In [1], the definition of periodic plus smooth decomposition was given as follows:

**Definition 1.** Let  $u \in \mathbb{R}^\Omega$  be a gray-level image, defined on a discrete rectangular domain  $\Omega$ . There exists a unique couple of images  $(p, s) \in (\mathbb{R}^\Omega)^2$  that minimizes

$$E(p, s) = \sum_{\substack{\mathbf{x} \in \Omega, \mathbf{y} \in \mathbb{Z}^2 \setminus \Omega, \\ |\mathbf{x} - \mathbf{y}|=1}} (p(\mathbf{x}) - p(\mathbf{y}))^2 + \sum_{\substack{\mathbf{x} \in \Omega, \mathbf{y} \in \Omega, \\ |\mathbf{x} - \mathbf{y}|=1}} (s(\mathbf{x}) - s(\mathbf{y}))^2$$

under the constraints

$$u = p + s, \quad \text{and} \quad \text{mean}(s) = 0,$$

where  $\dot{\mathbf{y}}$  is the unique element of  $\Omega$  equal to  $\mathbf{y}$  modulo  $\Omega$ , and

$$\text{mean}(s) = \frac{1}{|\Omega|} \sum_{\mathbf{x} \in \Omega} s(\mathbf{x}).$$

The image  $p$  is to be called the periodic component of  $u$  (also written  $\text{per}(u)$ ) and  $s$  the smooth component of  $u$ .



Figure 1: Original images and its periodic

## 2.1 Strong aliasing scenario (direct subsampling)

The key idea in image sub-sampling is to throw away every other row and column to create a half-size image. When the sampling rate gets too low, we are not able to capture the details in the image anymore.

To reduce the dimension, we apply:

$$g(i, j)_{\begin{subarray}{l} 0 \leq i \leq \frac{N}{2} \\ 0 \leq j \leq \frac{N}{2} \end{subarray}} = f(2i, 2j) \quad (2)$$

The figure 2 shows us directly subsampled image presents strong aliasing artifacts. At spatial domain, the result has many aliasing at plaid details. And in Fourier domain, aliasing appears at the four corner of images. Looking at the picture Fourier transform of reduction image, we see that the high-frequency pattern change the direction as well as the frequency.

## 2.2 Light aliasing scenario without no frequency cut off

In Fourier domain, we multiply a Gaussian kernel such that  $\varphi(0) = 1$  and  $\varphi(f, 0) = \varphi(0, f) = e^{-1/2}$ , where  $f$  is the cut-off frequency. Gaussian kernel is defined as:

$$G(x, y) = \frac{1}{2\pi\sigma^2} e^{-\frac{x^2+y^2}{2\sigma^2}}. \quad (3)$$

Next, we downsample the image of factor  $z$ . In this report, we choose  $z = 2$ .

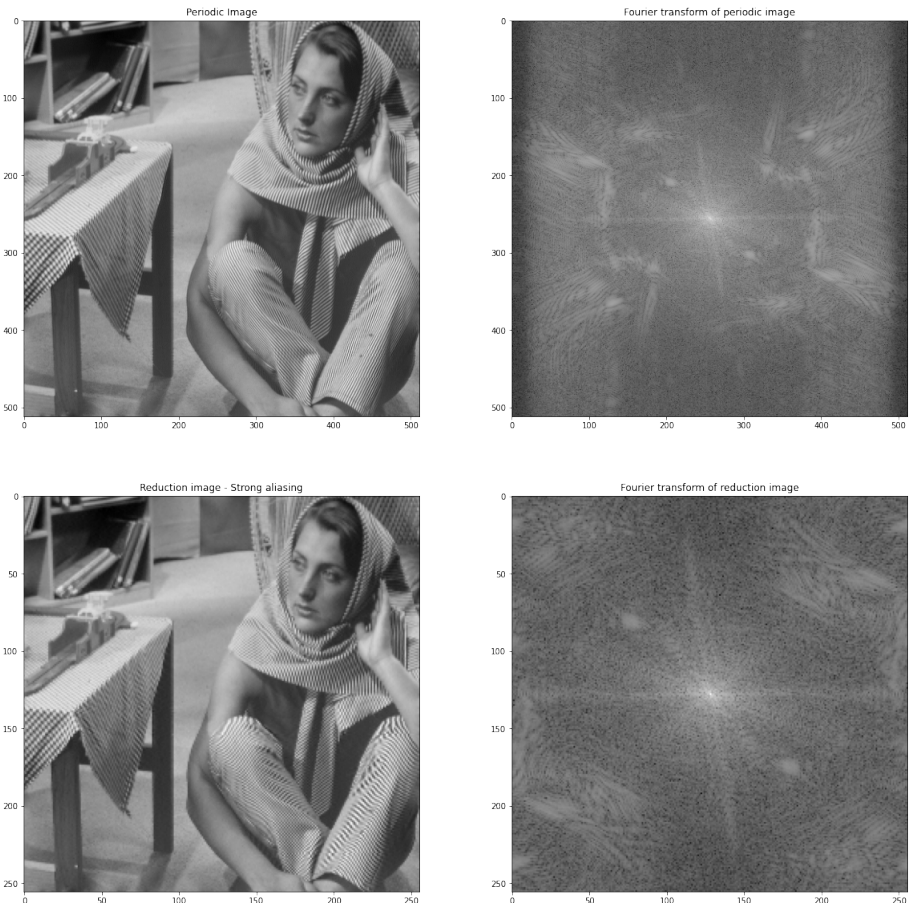


Figure 2: Periodic image and its Fourier domain after applying direct subsampling

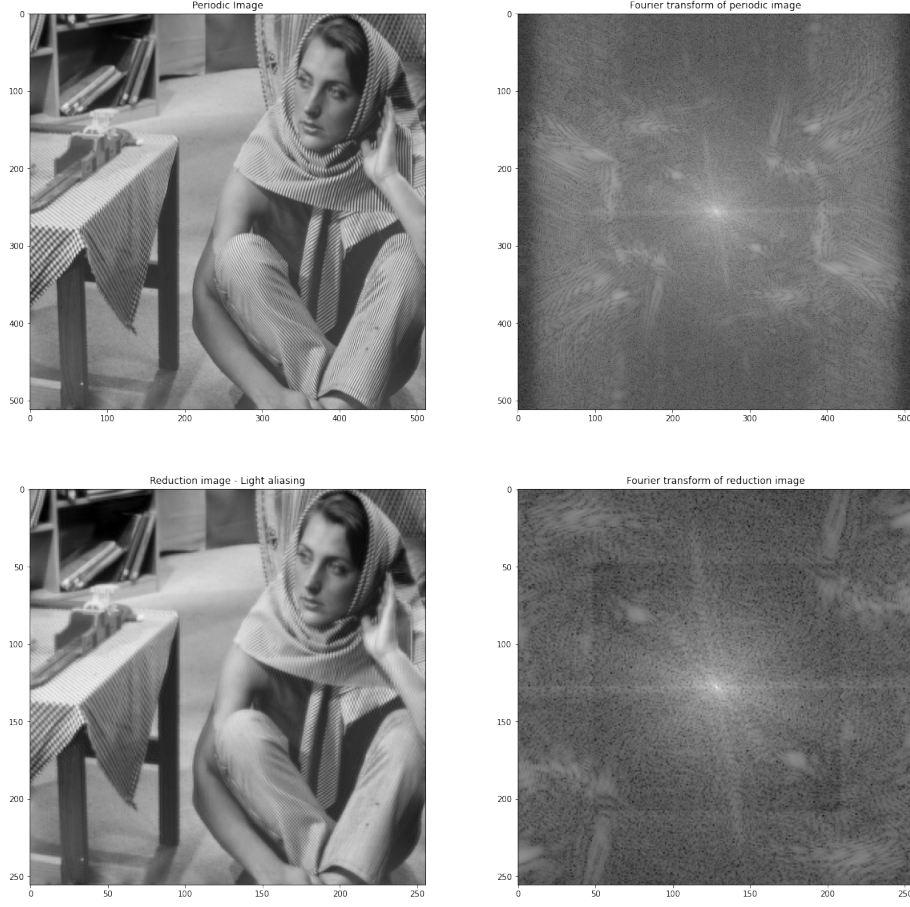


Figure 3: Periodic image and its Fourier domain after performing with light aliasing scenario

### 2.3 No aliasing scenario with hard frequency cut off

Shannon theorem tells us how to avoid aliasing: ideally we should perform a perfect frequency cutoff, by transforming the geometrical image  $u$  into an image  $v$  such that

$$\hat{v} = \hat{u} \cdot 1_{\left[-\frac{\pi}{\gamma}, \frac{\pi}{\gamma}\right]^2}. \quad (4)$$

A hard frequency cutoff (equation (4), that is a projection on Shannon condition, may be realized as a direct application of the Fourier model. This corresponds to the projection on band-limited signals with a given resolution. However, a hard frequency cutoff has an important drawback: since it corresponds to a sinc convolution in spatial domain, it produces ringing around edges.

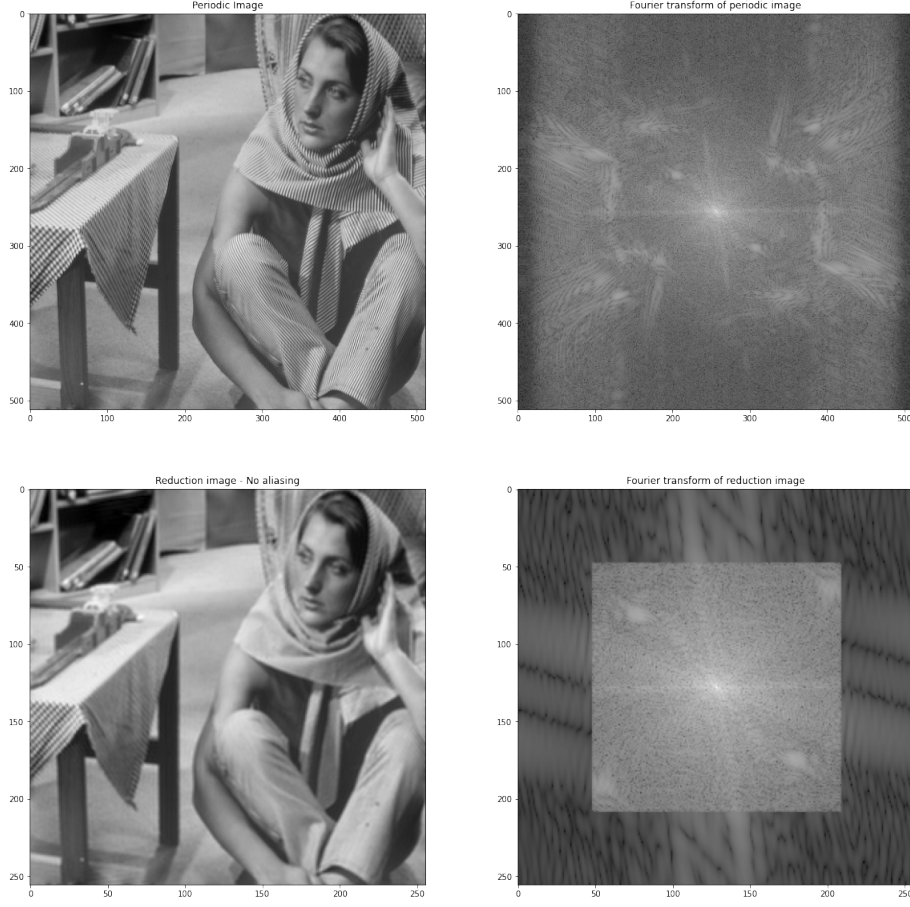


Figure 4: Periodic image and its Fourier domain after performing with no aliasing scenario

### 3 Registration methods

#### 3.1 Bilinear interpolation

First of all, we would like to investigate the translation of the image by using the bilinear interpolation. Let us denote  $F$  stand for the bilinear interpolation of the image  $f$  shifted by the translation  $t = (\delta_x, \delta_y)$ . Our goal is to find the optimal translation  $(\delta_x, \delta_y)$  such that:

$$\min_{\delta_x, \delta_y} \sum_{k,l} (F(k - \delta_x, l - \delta_y) - g(k, l))^2 \quad (5)$$

Let us note that in this case, we can find the explicit solution for the least square problem. In particular, by using the definition of the bilinear interpolation, we obtain

$$\begin{aligned} & F(k - \delta_x, l - \delta_y) - g(k, l) \\ &= \delta_x \delta_y f(k-1, l-1) + \delta_x (1 - \delta_y) f(k-1, l) + (1 - \delta_x) \delta_y f(k, l-1) + (1 - \delta_x)(1 - \delta_y) f(k, l) - g(k, l) \\ &= \delta_x \delta_y f_{k-1, l-1} + \delta_x f_{k-1, l} - \delta_x \delta_y f_{k-1, l} + \delta_y f_{k, l-1} - \delta_x \delta_y f_{k, l-1} + f_{k, l} - \delta_y f_{k, l} - \delta_x f_{k, l} + \delta_x \delta_y f_{k, l} - g_{k, l} \\ &= \delta_x \delta_y (f_{k-1, l-1} - f_{k-1, l} - f_{k, l-1} + f_{k, l}) + \delta_x (f_{k-1, l} - f_{k, l}) + \delta_y (f_{k, l-1} - f_{k, l}) + f_{k, l} - g_{k, l} \end{aligned}$$

Then, it is useful to see that the optimization problem (5) is equivalent to

$$\min \mathcal{L}(\beta) := \|X\beta - Y\|^2 = Y^\top Y - Y^\top X\beta - \beta^\top X^\top Y + \beta^\top X^\top X\beta \quad (6)$$

where

$$X = \begin{pmatrix} f_{-1,0} - f_{0,0} & f_{0,-1} - f_{0,0} & f_{-1,-1} - f_{-1,0} - f_{0,-1} + f_{0,0} \\ \vdots & \vdots & \vdots \\ f_{k-1,l} - f_{k,l} & f_{k,l-1} - f_{k,l} & f_{k-1,l-1} - f_{k-1,l} - f_{k,l-1} + f_{k,l} \\ \vdots & \vdots & \vdots \\ f_{M-2,N-1} - f_{M-1,N-1} & f_{M-1,N-2} - f_{M-1,N-1} & f_{M-2,N-2} - f_{M-2,N-1} - f_{M-1,N-2} + f_{M-1,N-1} \end{pmatrix}$$

and

$$\beta = \begin{pmatrix} \delta_x \\ \delta_y \\ \delta_x \delta_y \end{pmatrix}, \quad Y = \begin{pmatrix} g_{0,0} - f_{0,0} \\ \vdots \\ g_{k,l} - f_{k,l} \\ \vdots \\ g_{M-1,N-1} - f_{M-1,N-1} \end{pmatrix}_{\substack{0 \leq k \leq M-1 \\ 0 \leq l \leq N-1}}$$

We also note that the minimum of (6) can be achieved through the gradient of the loss function given by

$$\frac{\partial \mathcal{L}(\beta)}{\partial \beta} = -2X^\top Y + 2X^\top X\beta$$

Setting the gradient of the loss function to zero and solving for  $\beta$  we could get

$$\hat{\beta} = (X^\top X)^{-1}(X^\top Y)$$

### 3.2 Shannon interpolation

To be convenient, we denote  $I_M = \{0, 1, \dots, M-1\}$  and  $I_N = \{0, 1, \dots, N-1\}$ , let define  $u : I_M \times I_N \rightarrow \mathbb{R}$  be a discrete  $M \times N$  image. Then, the DFT  $\hat{u} : \mathbb{Z}^2 \rightarrow \mathbb{C}$  is defined by

$$\hat{u}(\alpha, \beta) = \sum_{k \in I_M, l \in I_N} u(k, l) e^{-2\pi i (\frac{\alpha k}{M} + \frac{\beta l}{N})}.$$

We also define the inverse DFT of  $\hat{u}$  for integer value  $x$  and  $y$  as

$$u(x, y) = \frac{1}{MN} \sum_{\alpha \in \hat{I}_M, \beta \in \hat{I}_N} \hat{u}(\alpha, \beta) e^{2\pi i (\frac{\alpha x}{M} + \frac{\beta y}{N})}.$$

where  $\hat{I}_M = [-\frac{M}{2}, \frac{M}{2}] \cap \mathbb{Z}$  and  $\hat{I}_N = [-\frac{N}{2}, \frac{N}{2}] \cap \mathbb{Z}$ .

**Definition 2.** The discrete Shannon interpolation of discrete image  $u : I_M \times I_N \rightarrow \mathbb{R}$  is  $U : \mathbb{R}^2 \rightarrow \mathbb{R}$  defined by

$$U(x, y) = \sum_{k \in I_M, l \in I_N} u(k, l) sincd_M(x - k) sincd_N(y - l) \quad (7)$$

where

$$sincd_M(x) = \begin{cases} \frac{\sin(\pi x)}{M \sin(\frac{\pi x}{M})} & \text{if } M \text{ is odd} \\ \frac{\sin(\pi x)}{M \tan(\frac{\pi x}{M})} & \text{if } M \text{ is even} \end{cases} \quad (8)$$

For an integer  $M$ , let us define

$$\varepsilon_M(\alpha) = \begin{cases} \frac{1}{2} & \text{if } |\alpha| = \frac{M}{2} \\ 1 & \text{otherwise} \end{cases} \quad (9)$$

According to [2], we have the following propositions

**Proposition 1.** *The discrete Shannon interpolation of discrete image  $u : I_M \times I_N \rightarrow \mathbb{R}$  can be written as*

$$U(x, y) = \frac{1}{MN} \sum_{\alpha \in \hat{I}_M, \beta \in \hat{I}_N} \varepsilon_M(\alpha) \varepsilon_N(\beta) \hat{u}(\alpha, \beta) e^{2\pi i (\frac{\alpha k}{M} + \frac{\beta l}{N})}$$

where  $\varepsilon_M(\alpha)$  and  $\varepsilon_N(\beta)$  is defined in (9).

**Proposition 2.** *The discrete Shannon interpolation of discrete image  $u : I_M \times I_N \rightarrow \mathbb{R}$  can be also written as*

$$U(x, y) = \Re \left( \frac{1}{MN} \sum_{\alpha \in \hat{I}_M, \beta \in \hat{I}_N} \hat{u}(\alpha, \beta) e^{2\pi i (\frac{\alpha k}{M} + \frac{\beta l}{N})} \right).$$

By using the fact that  $(F(k - \delta_x, l - \delta_y) - g(k, l))^2 = F^2(k - \delta_x, l - \delta_y) - 2F(k - \delta_x, l - \delta_y)g(k, l) + g^2(k, l)$ , the optimization problem (5) becomes

$$\min_{\delta_x, \delta_y} \sum_{k, l} (F^2(k - \delta_x, l - \delta_y) - 2F(k - \delta_x, l - \delta_y)g(k, l)) \quad (10)$$

Let us define  $T_\delta f(k, l) = F(k - \delta_x, l - \delta_y)$  where  $F$  is a discrete Shannon interpolation of discrete image  $f$ , we obtain

$$\begin{aligned} T_\delta f(k, l) &= F(k - \delta_x, l - \delta_y) = \frac{1}{NM} \sum_{\alpha \in \hat{I}_M} \sum_{\beta \in \hat{I}_N} \hat{f}(\alpha, \beta) e^{2i\pi \left( \frac{\alpha(k - \delta_x)}{M} + \frac{\beta(l - \delta_y)}{N} \right)} \\ &= \frac{1}{NM} \sum_{\alpha \in \hat{I}_M} \sum_{\beta \in \hat{I}_N} \hat{f}(\alpha, \beta) e^{2i\pi \left( \frac{\alpha k}{M} + \frac{\beta l}{N} \right)} e^{-2i\pi \left( \frac{\alpha \delta_x}{M} + \frac{\beta \delta_y}{N} \right)} \end{aligned}$$

which implies that Fourier coefficients of  $T_\delta f$  can be written as

$$\widehat{T_\delta f}(\alpha, \beta) = \hat{f}(\alpha, \beta) e^{-2i\pi \left( \frac{\alpha \delta_x}{M} + \frac{\beta \delta_y}{N} \right)}.$$

Based on Parseval's identity, we have:

$$\|T_\delta f\|^2 = \sum_{\alpha, \beta} \left| \widehat{T_\delta f}(\alpha, \beta) \right|^2 = \sum_{\alpha, \beta} \left| \hat{f}(\alpha, \beta) e^{-2i\pi \left( \frac{\alpha \delta_x}{M} + \frac{\beta \delta_y}{N} \right)} \right|^2 = \sum_{\alpha, \beta} \left| \hat{f}(\alpha, \beta) \right|^2 = \|f\|^2$$

Therefore, we can say that the Shannon interpolation is able to translate image without the information loss. In order words,  $\sum_{k, l} F^2(k - \delta_x, l - \delta_y)$  not depend on  $\delta_x, \delta_y$ , then we have the problem (10) is equivalent to

$$\max_{\delta_x, \delta_y} \sum_{k, l} F(k - \delta_x, l - \delta_y)g(k, l) \quad (11)$$

The cross correlation between image  $f$  and  $g$  defined as follow

$$\omega = r_{fg}(\delta_x, \delta_y) = f \star g \quad (12)$$

We have  $\mathcal{F}(\omega) = \mathcal{F}(f).\mathcal{F}(g)^*$ . Therefore, applying the inverse Fourier transform (denote  $\mathcal{F}^{-1}$ ), we obtain

$$\begin{aligned}\mathcal{F}^{-1}\{\mathcal{F}(f).\mathcal{F}(g)^*\} &= \frac{1}{MN} \sum_{\alpha \in \hat{I}_M, \beta \in \hat{I}_N} \hat{f}(\alpha, \beta) \hat{g}^*(\alpha, \beta) e^{2\pi i(\frac{\alpha x}{M} + \frac{\beta y}{N})} \\ &= \frac{1}{MN} \sum_{\alpha \in \hat{I}_M, \beta \in \hat{I}_N} |\hat{f}(\alpha, \beta)|^2 e^{2i\pi(\frac{\alpha \delta_x}{M} + \frac{\beta \delta_y}{N})} e^{2\pi i(\frac{\alpha x}{M} + \frac{\beta y}{N})}\end{aligned}$$

Thus, it requires solving a general problem of subpixel image registration by locating the peak of the cross correlation.

$$[\delta_x, \delta_y] = \underset{x, y}{\operatorname{argmax}} (\mathcal{F}^{-1}\{\mathcal{F}(f).\mathcal{F}(g)^*\}) \quad (13)$$

Moreover, we can see that

$$P(\alpha, \beta) = \frac{\hat{f}(\alpha, \beta) \hat{g}^*(\alpha, \beta)}{|\hat{f}(\alpha, \beta) \hat{g}^*(\alpha, \beta)|} = e^{2i\pi(\frac{\alpha \delta_x}{M} + \frac{\beta \delta_y}{N})}$$

which leads to

$$\mathcal{F}^{-1}\{P(\alpha, \beta)\} = \mathcal{F}^{-1}\left\{e^{2i\pi(\frac{\alpha \delta_x}{M} + \frac{\beta \delta_y}{N})}\right\} = \delta(\delta_x, \delta_y)$$

As a result, we have

$$[\delta_x, \delta_y] = \underset{x, y}{\operatorname{argmax}} \left( \mathcal{F}^{-1} \left\{ \frac{\mathcal{F}(f).\mathcal{F}(g)^*}{|\mathcal{F}(f).\mathcal{F}(g)^*|} \right\} \right) \quad (14)$$

Since we only consider the translation between two images the general algorithm is to compute the upsampled cross correlation between two images by using fast Fourier transform (FFT) and locate its peak. In particular, we study the algorithm 1 for the image registration.

---

**Algorithm 1:** Subpixel image registration algorithm

---

**Input:** The cross correlation between image  $f$  and  $g$

**Output:** The location  $(\delta_x, \delta_y)$ .

- 1 **begin**
- 2    Compute the upsampled cross correlation  $W$  with zoom factor  $z$  by using the Shannon interpolation
- 3    Verify the initial peak estimate  $(k_0, l_0)$  where  $W$  is maximal
- 4    Solving the least square problem to find an approximation of  $W$  around  $(k_0, l_0)$  under the following polynomial form:

$$\tilde{W}(x, y) = a_1 x^2 + a_2 x y + a_3 y^2 + a_4 x + a_5 y + a_6$$

- 5    Find explicit the maximizer  $(\bar{x}, \bar{y})$  of  $\tilde{W}$  by Solving the linear system  $\nabla \tilde{W} = 0$ :

$$\begin{pmatrix} 2a_1 & a_2 \\ a_2 & 2a_3 \end{pmatrix} \begin{pmatrix} x \\ y \end{pmatrix} = - \begin{pmatrix} a_4 \\ a_5 \end{pmatrix}$$

The peak location is given by

$$(\delta_x, \delta_y) = \frac{(k_0, l_0) + (\bar{x}, \bar{y}) - (k_c, l_c)}{z}$$

where  $(k_c, l_c)$  is a center position of  $W$

---

Let us also note that there are several algorithm to find the subpixel image registration. For instance, according to [3], we can iteratively search for the image displacement  $(\delta_x, \delta_y)$  which maximize the cross correlation by using the nonlinear optimization conjugate gradient or the single step DFT approach: an upsampled cross correlation by factor in only computed in a  $1.5 \times 1.5$  pixel neighborhood about the initial estimate. Moreover, we would like to mention the Iterative Phase Correlation (IPC) algorithm introduced in [4]. This is an extension of the well known phase correlation method.

## 4 Numerical results

In this part, we present some test case with all reduction and registration methods. By using 100 random couples of translation  $t = (t_x, t_y)$ , we test three registration methods with reduced periodic images and reduced noisy images.

### 4.1 The recurrent testing pattern

The recurrent testing pattern in this project will be the following:

1. Take a well-sampled image and extract its periodic component  $u_0$ .
2. Pick a random translation  $t \in [0, \frac{1}{2}]^2$ .
3. Apply a periodic translation of vector  $z \cdot t$  to  $u_0$  to obtain an image  $u_1$ .
4. Apply one of reduction methods in section 2 to transform  $u_0$  and  $u_1$  into reduced images  $v_0$  and  $v_1$ .
5. Add a white Gaussian noise with standard deviation  $\sigma$  to  $v_0$  and  $v_1$ , which gives images  $w_0$  and  $w_1$ .
6. Apply registration methods in section 3 to estimate the translation  $\tilde{t}$  between  $w_0$  and  $w_1$ .
7. Compute the error  $\|\tilde{t} - t\|^2$ .

This process will be iterated over a lot of random translation to estimate an error map (average square error  $\|\tilde{t} - t\|^2$  as a function of  $t$ ).

### 4.2 Test case with bilinear interpolation

In this part, we give two test case: one for a periodic image and other for noisy images. Each case, we take 100 random samples  $t \in [0, \frac{1}{2}]^2$  and generate a graph with list of errors for strong, light and no aliasing.

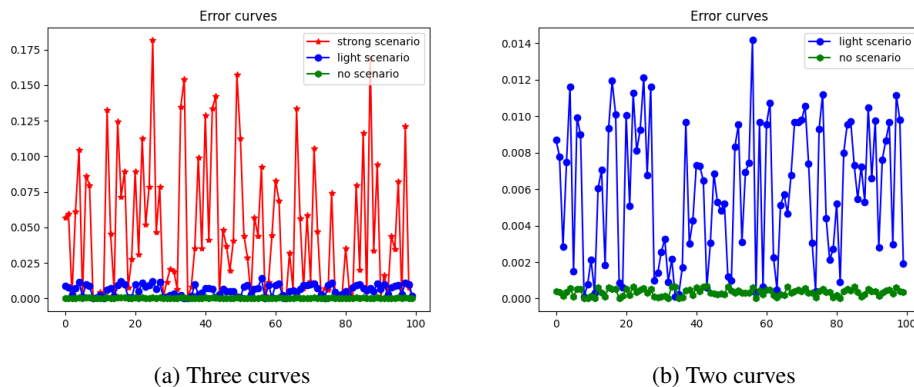


Figure 5: Error curves  $\|\tilde{t} - t\|^2$  with registration methods by applying bilinear interpolation (periodic image)

For noisy images, we choose  $\sigma_{\text{noise}} = 0.05 \max(u_0)$

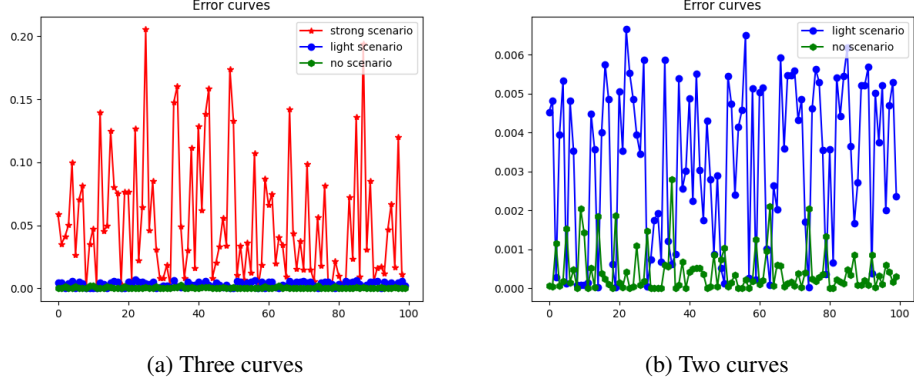


Figure 6: Error curves  $\|\tilde{t} - t\|^2$  with registration methods by applying bilinear interpolation (noisy image)

From the figure 5 and 6, in general, error between  $\tilde{t}$  and  $t$  is descent with strong, light, no aliasing, respectively. Bilinear interpolation approximates the translation is quite well for slight and no aliasing. Meanwhile, when we add Gaussian noise into the reduced images, the error is higher than the one having no noise by observing and comparing figure 5a and figure 6a, figure 5b and figure 6b.

#### 4.3 Test case with Shannon interpolation

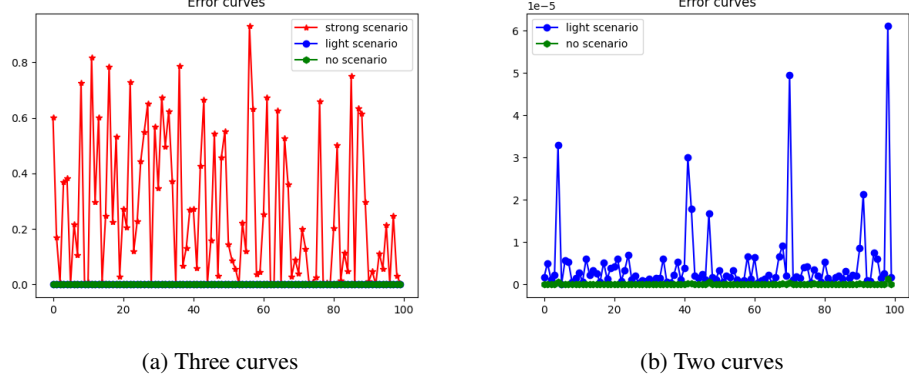


Figure 7: Error curves  $\|\tilde{t} - t\|^2$  with registration methods by applying Shannon interpolation (periodic image)

For noisy images, we choose  $\sigma_{\text{noise}} = 0.05 \max(u_0)$

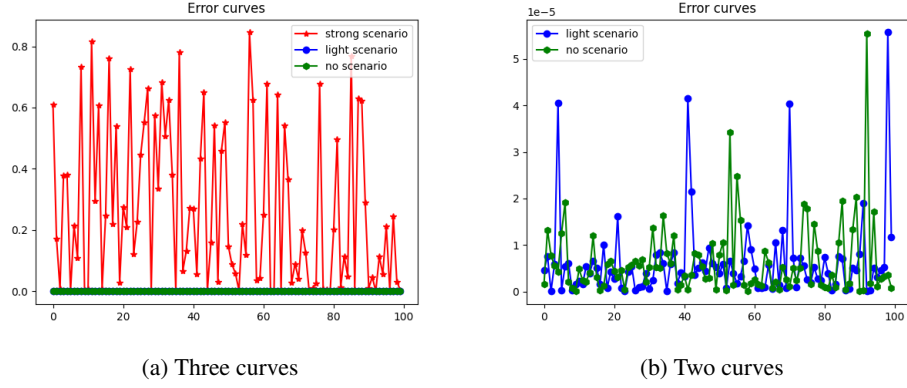


Figure 8: Error curves  $\|\tilde{t} - t\|^2$  with registration methods by applying Shannon interpolation (noisy image)

For Shannon interpolation, the strong scenario also gives the highest error and decreases to light aliasing and no aliasing. Observing figure 7a and 8a, we realized there is no change when adding Gaussian noise to reduced images. In contrast, with no aliasing, when we add noise, the error also higher than that one having no noise (figure 7b and 8b). Compare the result of Shannon interpolation to the one of bilinear interpolation, it implies that bilinear interpolation gives the result better in strong scenario but Shannon interpolation has the accuracy more accurate in light and no scenario. To improve the performance of Shannon interpolation on strong aliasing images, we can use Gaussian smoothing.

#### 4.4 Test case with Shannon interpolation and Gaussian smoothing

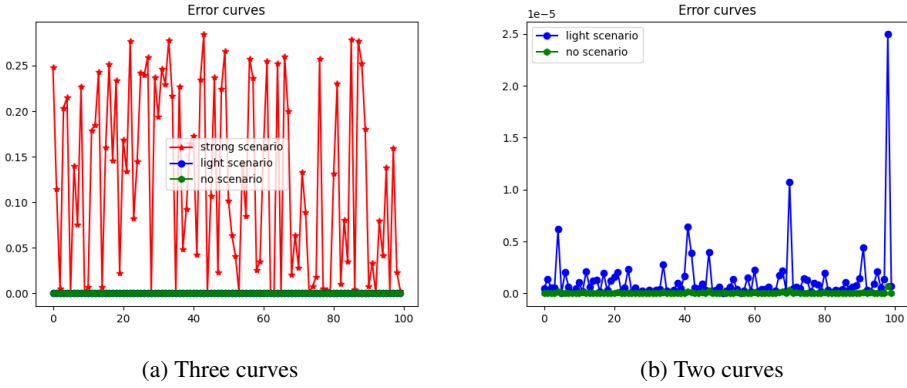


Figure 9: Error curves  $\|\tilde{t} - t\|^2$  with registration methods by applying Shannon interpolation and Gaussian smoothing (periodic image)

For noisy images, we choose  $\sigma_{\text{noise}} = 0.05 \max(u_0)$

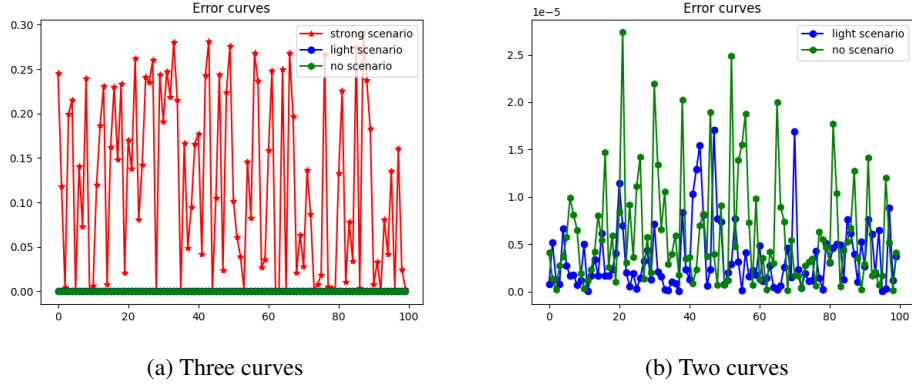


Figure 10: Error curves  $\|\tilde{t} - t\|^2$  with registration methods by applying Shannon interpolation and Gaussian smoothing (noisy image)

With Gaussian smoothing, we choose  $\sigma = 1$  and the performance on strong scenario has improved comparing to the result was used only Shannon interpolation. For light and no scenario, the result is quite same as the one when only using Shannon interpolation, the value of error is also lower. However, depend on choosing  $\sigma$  of Gaussian smoothing that leads to the performance. If we choose  $\sigma$  is too small, the performance will not improved too much. Therefore, we need to choose a  $\sigma$  good enough.

5 Conclusion

In this project, we know some reduction methods which helps reduce the dimensionality of data. Depend on each method that aliasing was created or not. Also, we implement some registration methods to estimate translation between reduced images and reduced shifted images with many case: aliasing, noise. Through performing the test cases, Shannon interpolation and Gaussian smoothing is the best method show us the highest accuracy for both no or having noise. In general, the error of registration methods is the highest for the images after applying direct subsampling has strong aliasing artifacts . This error is lower for light and lowest for no aliasing. Besides that, we also perceive the effect of noise when implementing registration methods. Almost the error when having noise is higher than the one having no noise.

## References

- [1] L. Moisan, Periodic plus smooth image decomposition, *Journal of Mathematical Imaging and Vision* 39 (2) (2011) 161–179.
  - [2] R. Abergel, L. Moisan, The shannon total variation, *Journal of Mathematical Imaging and Vision* 59 (2) (2017) 341–370.
  - [3] M. Guizar-Sicairos, S. T. Thurman, J. R. Fienup, Efficient subpixel image registration algorithms, *Optics letters* 33 (2) (2008) 156–158.
  - [4] Z. Hrazdíra, M. Druckmüller, S. Habbal, Iterative phase correlation algorithm for high-precision subpixel image registration, *The Astrophysical Journal Supplement Series* 247 (1) (2020) 8.